Journal of Power and Energy Engineering, 2023, 11, 18-28
https://www.scirp.org/journal/jpee
ISSN Online: 2327-5901
ISSN Print: 2327-588X

Harmonic Resonance Analysis of Shale Gas Distribution Network with Phased Load

Zhongjian Kang, Lei Li

College of New Energy, China University of Petroleum (East China), Qingdao, China
Email: hbzjklilei@163.com

How to cite this paper: Kang, Z.J. and Li, L. (2023) Harmonic Resonance Analysis of Shale Gas Distribution Network with Phased Load. *Journal of Power and Energy Engineering*, **11**, 18-28.
https://doi.org/10.4236/jpee.2023.111002

Received: January 2, 2023
Accepted: January 28, 2023
Published: January 31, 2023

Abstract

Based on the background of achieving carbon peaking and carbon neutrality, the development and application of new high-power compressors, electric grid drilling RIGS and electric fracturing pump system provide new equipment support for the electric, green and intelligent development of shale gas fields in China. However, the harmonic pollution of shale gas grid becomes more serious due to the converter and frequency conversion device in the system, which easily causes harmonic resonance problem. Therefore, the harmonic resonance of shale gas grid is comprehensively analyzed and treated. Firstly, the working mechanism of compressor, electric drilling RIGS of the harmonic impedance model of electric fracturing pump system is established. Secondly, the main research methods of harmonic resonance analysis are introduced, and the basic principle of modal analysis is explained. Modal analysis method was used to analyze. Finally, harmonic resonance is suppressed. The results show that there may be multiple resonant frequency points in the distribution network changes, but these changes are relatively clear; if the original resonant frequency point of the resonant loop does not exist, the resonant frequency point disappears. The optimal configuration strategy of passive filter can effectively suppress harmonic resonance of distribution network in shale gas field.

Keywords

Shale Gas Distribution Grid, Harmonic Resonance, Modal Analysis Method, Active Power Filter

1. Introduction

According to statistics, China's shale gas reserves account for about 1/5 of the world, which has good exploration and development prospects [1]. In recent years, with the use of a large number of electronic power equipment and the continuous expansion of distribution network, the harmonic resonance problem of oil distribution network is becoming more and more serious. In view of these harmonic resonance problems, domestic and foreign experts and scholars have carried out a series of research work [2]-[9]. In reference [10], modal analysis method is used to obtain various information of resonance when wind power plants are connected to the grid, which proves that the harmonic resonance modal analysis method is also applicable in distributed power grid. In reference [11], the harmonic resonance problem of multi-inverter system was analyzed. It was found by modal analysis that only some components had a great influence on the resonant mode. In literature [12] [13], modal analysis method and virtual branch method are applied to combine circuit impedance matrix, virtual branch method and modal analysis method, and then the series harmonic resonance is analyzed, and a complete analysis result on harmonic resonance is obtained.

For oil field with variable frequency device in the power grid equipment is easy to cause resonance problem such as fracturing and oil field in this paper, the power grid harmonic resonance fault mechanism research; using modal analysis method of easy cause harmonic resonance area monitoring, research results can eliminate interference to electric network load running, to ensure the stability of the power grid. It has a broad application prospect in harmonic resonance monitoring and suppression of oil power grid.

2. Working Principle of Harmonic Source in Grid of Shale Gas Field

The use of frequency conversion and current conversion devices in the periodic loads of shale gas field, such as high-power compressor, grid electric drill and electric fracturing pump, makes the harmonic pollution problem of the distribution network of shale gas field more serious. The working principle and harmonic characteristics of the 6 pulse and 36 pulse wave rectifier are analyzed to lay the foundation for the harmonic resonance analysis.

2.1. Working Principle of Frequency Converter of Grid Electric Drill

Variable-frequency Drive (VFD) is a power control device that uses frequency conversion technology and microelectronic technology to control AC motors by changing the frequency mode of motor working power supply. The topology of 6 pulse frequency converter is shown in **Figure 1**.

The topology of the inverter can be a diode clamp (NPC) three-level structure, and the motor control is V/F control strategy. Its technology is widely used, and a large amount of product application experience can be used, which is very important to ensure the reliability of the fracturing system [10].

The inverter control adopted includes speed control and space vector regulation, and the V/F control block diagram is shown in **Figure 2**.

The input active power of the induction motor is:

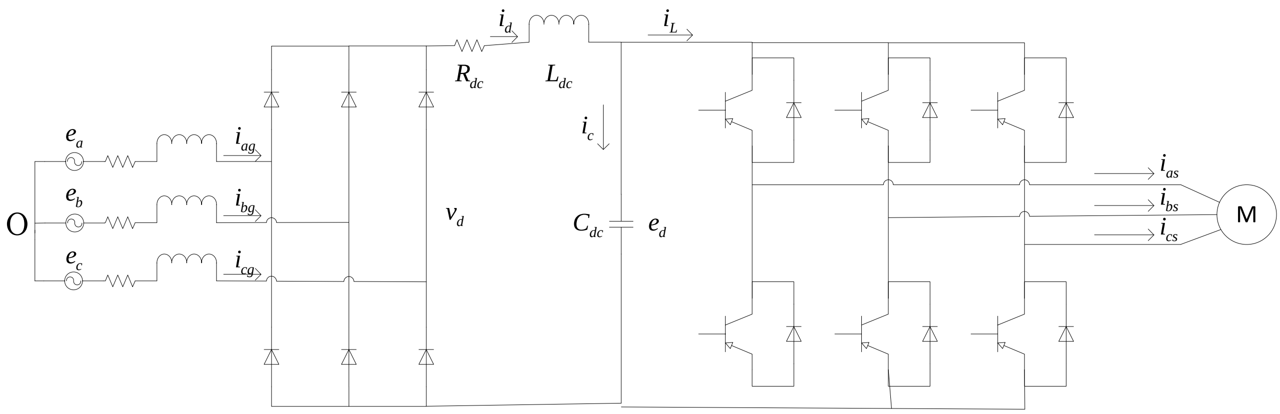

Figure 1. Topology of 6 pulse frequency converter.

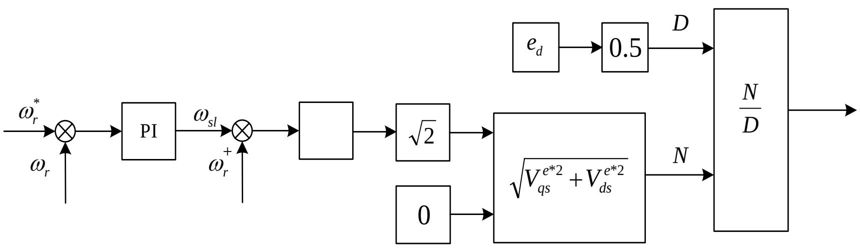

Figure 2. Mathematical logic diagram of V/F control.

$$P_{IM} = \frac{3}{2}(v_{ds}i_{ds} + v_{qs}i_{ds}) \tag{1}$$

The input power of the inverter is:

$$P_{IN} = e_d i_l \tag{2}$$

2.2. Working Principle of Frequency Converter of Electric Fracturing Pump

The main requirements of fracturing pump equipment are high pressure, large displacement, large scale and long working time [11]. Therefore, the single horsepower is large and requires a high degree of reliability. The fracturing pump generally adopts the intermittent working system, such as continuous work, the average working pressure ratio is generally required to not exceed 60%, and the average power utilization rate is not more than 60%.

The main circuit structure of the frequency converter used in the electric drive system of the fracturing pump is a six-phase motor scheme with a series 36 pulse wave diode uncontrolled rectifier and a diode-clamped three-level topological inverter bridge. The main circuit topology is shown in **Figure 3**.

The circuit structure shown in **Figure 3** is mainly composed of a three-phase 10 kV voltage source u_0, a 36-pulse phase shifting transformer T, six three-phase uncontrolled rectifiers (including B1 and B2 in series, B3 and B4 in series, B5 and B6 in series), three three-level NPC inverters N_1, N_2, N_3 and a six-phase asynchronous motor. The front six 6-pulse uncontrolled rectifiers are powered

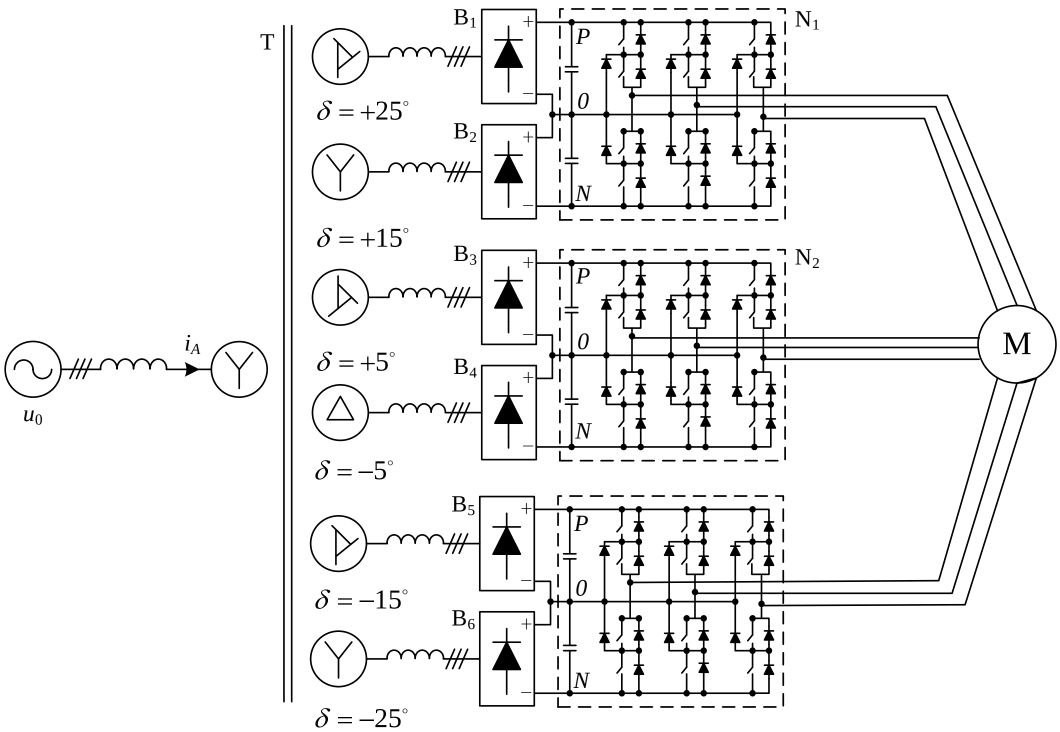

Figure 3. Main circuit of electric fracturing pump system.

by a 36-pulse phase-shifting transformer with six side-side winders in cascade to reduce the side harmonics. The rectifier output in series realizes the set value of the bus voltage, where point O is connected to the neutral point of the NPC three levels to realize the hardware clamp of the midpoint voltage.

Through mathematical derivation, the general formula of rectifier circuit is obtained:

$$u_{da} = U_{d0}[1 - \sum_{n=mk}^{\infty} \frac{2\cos k\pi}{2n-1} \cos n\omega t] \tag{3}$$

When $m = 2$, plug in the formula

$$u_{da} = \sqrt{2}u_2 \frac{2}{\pi} \sin\frac{\pi}{2}[1 + \frac{2}{2\times 4}\cos 2\omega t + \frac{2}{3\times 5}\cos 4\omega t + \frac{2}{5\times 7}\cos 6\omega t + \Lambda] \tag{4}$$

When $m = 6$, plug in the formula

$$\begin{aligned} u_{da} = \sqrt{2}u_{2L} \frac{6}{\pi}\sin\frac{\pi}{6}[1 + \frac{2}{5\times 7}\cos 6\omega t + \frac{2}{11\times 13}\cos 12\omega t \\ + \frac{2}{17\times 19}\cos 18\omega t + \frac{2}{23\times 25}\cos 24\omega t + \Lambda] \end{aligned} \tag{5}$$

From the 12 pulse wave rectifier Fourier series expansion, we can see two rectifier Bridges, harmonics cancel each other, leaving only 12 K ± 1 times, K is a positive integer, only 36 ± 1 times for 36 pulse wave, 36 pulse wave above the suppression of harmonic has not much effect, so the choice of 36 pulse wave, can get the maximum cost performance.

After being connected to the hydraulic fracturing pump system, the total harmonic distortion rate of the AC side current is 3.49%, and the content of the 35th and 37th harmonics of the higher harmonics is 0.21% and 0.22%, respectively. The total harmonic distortion rate of voltage is 3.55%, but the harmonic frequency distribution characteristics are different from the current. The content of the subharmonics in the low voltage is generally lower than that in the current, and the main harmonic components are concentrated in the 35th and 37th. Under certain conditions, the harmonic components of some frequencies will increase and the phenomenon of harmonic oscillation will occur.

3. Harmonic Resonance Analysis of Grid in Shale Gas Field

3.1. Theoretical Analysis of Harmonic Resonance

In an AC circuit containing resistors, inductors and capacitors, the voltage and current at both ends of the circuit are generally different. If the circuit parameters or the power supply frequency make the current and the power supply voltage the same, the circuit is resistive, and this state becomes resonant [12]. Resonance can be divided into series resonance and parallel resonance, parallel resonance generally occurs in the power system distribution network. The simple resonant loop is shown in **Figure 4**.

The circuit impedance value in **Figure 6** is as follows.

$$Z = \frac{(R + j\omega L)\frac{1}{j\omega C}}{R + j\omega L + \frac{1}{j\omega C}} = \frac{1}{\frac{CR}{L} + j(\omega C - \frac{1}{\omega L})} \quad (6)$$

If the circuit is resonant, I and U must be in phase, and the total reactance of the circuit is zero. At this time, the impedance is maximum when the circuit is resonant in parallel:

$$Z = \frac{L}{CR} \quad (7)$$

The resonant frequency is:

$$f_0 = \frac{1}{2\pi\sqrt{LC}} \quad (8)$$

According to the above equation, the larger the product of inductance L and capacitance C in the circuit, the smaller the resonant frequency.

3.2. Harmonic Resonant Mode Analysis of Grid for Shale Gas Field

For the modal analysis method of distribution network in shale gas field, the

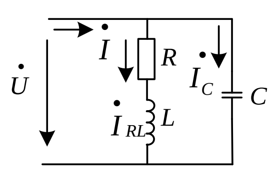

Figure 4. Harmonic resonance loop.

resonant frequency point is determined by scanning the modal impedance, and the feature vector and participation factor are determined to monitor and suppress the resonant problem [13].

The steps of modal analysis method for distribution network of shale gas field are as follows:

1) The eigenvalues are arranged in ascending order according to their size, and the eigenvalue matrix of the admittance matrix of the distribution network node under the determined resonant frequency is obtained, as shown in Equation (9).

$$\begin{bmatrix} \lambda_1 & 0 & 0 & 0 \\ 0 & \lambda_2 & 0 & 0 \\ 0 & 0 & \cdots & 0 \\ 0 & 0 & 0 & \lambda_n \end{bmatrix} \rightarrow \begin{bmatrix} \lambda_i \\ \lambda_j \\ \cdots \\ \lambda_p \end{bmatrix} \tag{9}$$

2) Find the feasible solution of the highest excitation node, that is, the key right eigenvectors corresponding to the first m minimum eigenvalues: [R_{i1}, R_{i2}, ..., R_{in}], [R_{j1}, R_{j2}, ..., R_{jn}]...

3) The mode with the largest impedance value (per unit value) in the feasible solution of the highest excitation node that resonates at the resonant frequency is found to be the key mode.

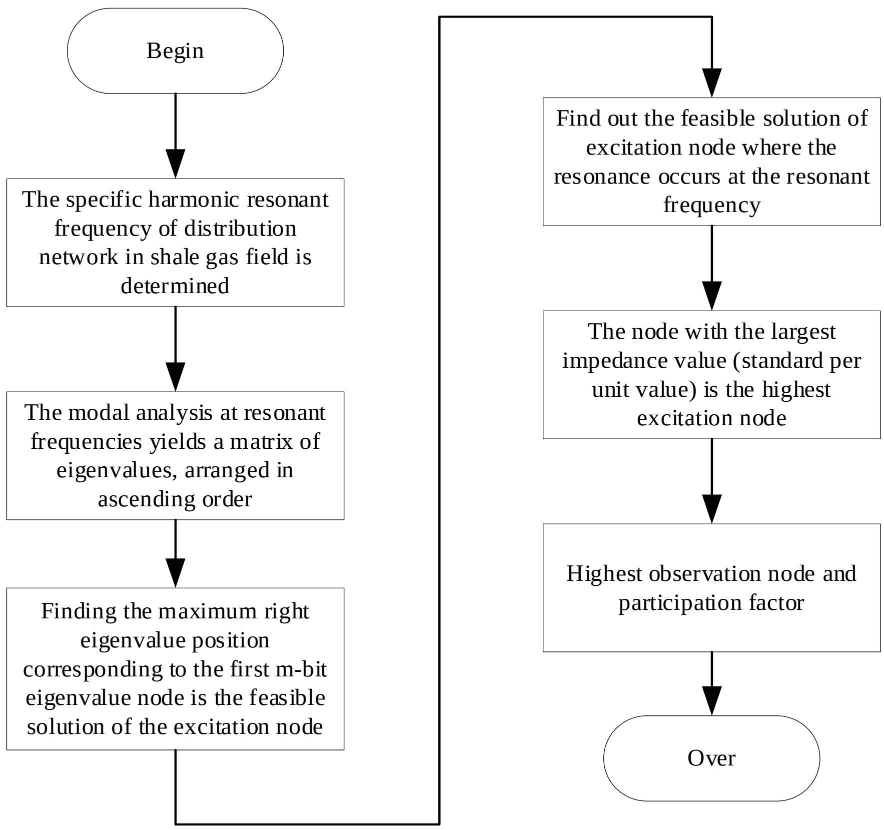

Figure 5. Calculation flow of modal analysis method for distribution network in shale gas field.

4) The highest observation node and the corresponding participation factor are determined by the key modes.

Figure 5 shows the calculation flow chart of mode analysis method for distribution network of shale gas field.

4. Analysis of Example

Taking the distribution network of a shale gas field as an example, the harmonic resonance problem in the distribution network of the shale gas field is analyzed. The distribution network of this shale gas field is shown in **Figure 6**. Through 220 kV, 110 kV and 110 kV substations, there are several branch lines under each line to supply power to each gas production, fracturing and drilling platform in turn.

4.1. Harmonic Resonance Analysis of Distribution Network in Shale Gas Field

Sweep the frequency of the distribution network of the entire shale gas field, and the simulation results are shown in **Figure 7** (the abscissa represents the frequency

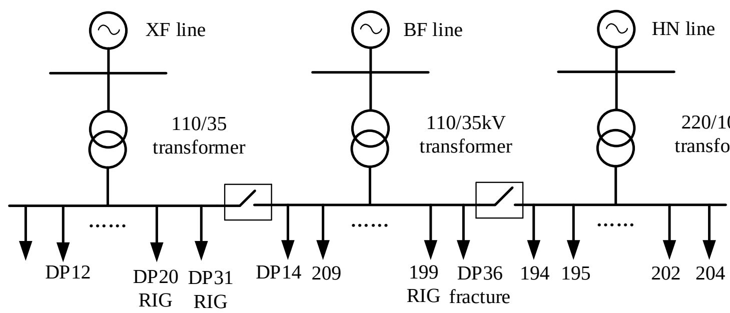

Figure 6. Schematic diagram of distribution network in shale gas field.

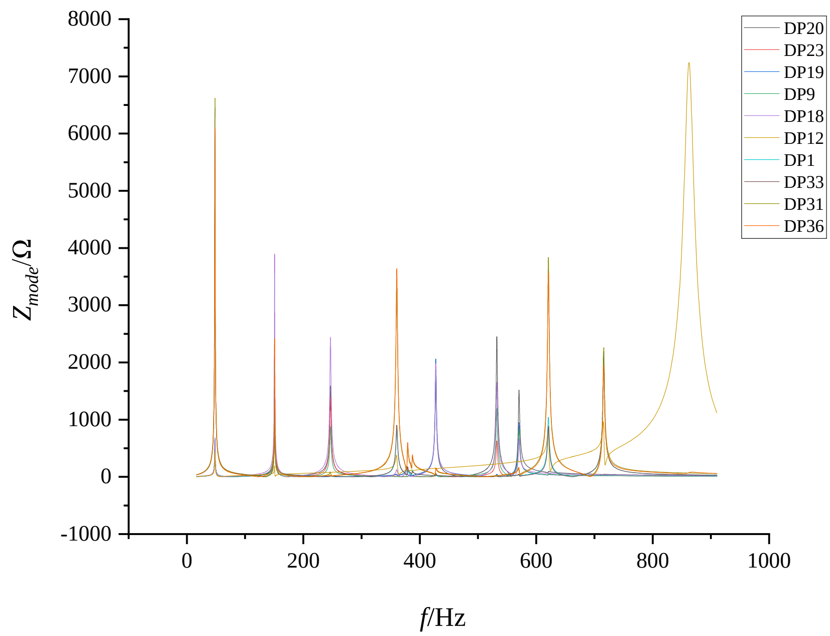

Figure 7. Harmonic resonance simulation diagram of distribution network in shale gas field.

/Hz, and the ordinate represents the impedance/Ω):

It can be seen from **Figure 7** that the resonant frequencies easily causing resonant overvoltage are determined to be 360 Hz, 532 Hz, 621 Hz and 1725 Hz for the 5, 7, 11, 13 and 35 harmonics in the grid of shale gas field, which are consistent with the results in **Table 1**.

4.2. Harmonic Resonance Analysis of Distribution Network in Shale Gas Field under Different Operating Conditions

In order to further avoid the occurrence of harmonic resonance, the resonant frequency points of different platforms in the distribution network of shale gas fields under the fracturing operation conditions were scanned.

1) The DP36 fracture was removed

The mode analysis method is used to analyze the harmonic resonance of the distribution network of the shale gas field after the removal of DP36 due to fault, and the frequency impedance characteristic curve is shown in **Figure 8**.

As can be seen from **Figure 8**, when the DP36 station fracturing is excised, there are three resonant frequency points in the frequency range of 0 - 1000 Hz, which are 158 Hz and 518 Hz and 719 Hz, respectively. It can be seen that the DP36 platform has a great influence on the 246 Hz, 425 Hz, 532 Hz and 573 Hz resonant frequency points, and the above resonant frequency points disappear after the removal of DP36. Among the three resonant frequency points, new 518 Hz and 719 Hz resonant frequency points appear in the remaining part of the distribution network of the shale gas field. The participating factors under the resonant frequency are analyzed, and the results are shown in **Table 1** and **Table 2**, respectively.

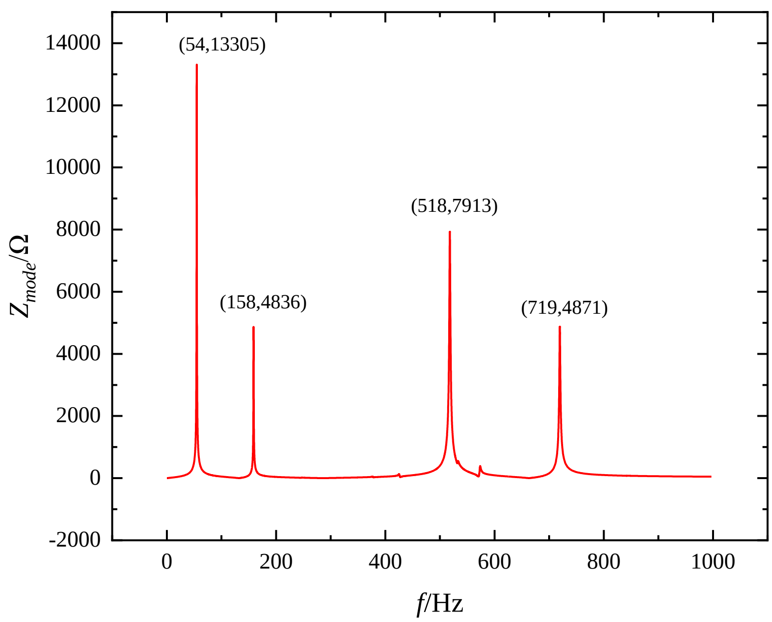

Figure 8. Z_{mode} scanning results of modal impedance characteristics of distribution network after removing electric fracturing pump of DP36 station.

Table 1. The main observation bus and excitation bus participation factors under 518 Hz (factor values are greater than 0.12).

Observation of bus	Bus voltage observation value/kV	Incentive bus	Bus voltage excitation value/kV	Participation factor
DP31	35	DP31	35	$0.1293\angle -3.75^{\circ}$
DP20	35	DP31	35	$0.1293\angle -3.75^{\circ}$
DP20	35	DP20	35	$0.1293\angle -3.75^{\circ}$
DP31	35	DP19	35	$0.1293\angle -3.75^{\circ}$
DP20	35	DP19	35	$0.1293\angle -3.75^{\circ}$
DP31	35	DP1	35	$0.1293\angle -3.75^{\circ}$
DP20	35	DP1	35	$0.1293\angle -3.75^{\circ}$
DP19	35	DP19	35	$0.1293\angle -3.75^{\circ}$
DP19	35	DP1	35	$0.1293\angle -3.75^{\circ}$
DP1	35	DP1	35	$0.1293\angle -3.75^{\circ}$
DP23	35	DP20	35	$0.1293\angle -4.04^{\circ}$
DP23	35	DP31	35	$0.1293\angle -4.04^{\circ}$
DP23	35	DP19	35	$0.1293\angle -4.04^{\circ}$
DP23	35	DP1	35	$0.1293\angle -4.04^{\circ}$
DP23	35	DP23	35	$0.1293\angle -4.32^{\circ}$

Table 2. The main observation bus and excitation bus participation factors under 719 Hz (factor values are greater than 0.11).

Observation of bus	Bus voltage observation value/kV	Incentive bus	Bus voltage excitation value/kV	Participation factor
DP31	35	DP31	35	$0.1183\angle -2.75^{\circ}$
DP18	35	DP31	35	$0.1183\angle -2.75^{\circ}$
DP18	35	DP18	35	$0.1183\angle -2.75^{\circ}$
DP31	35	DP19	35	$0.1183\angle -2.75^{\circ}$
DP18	35	DP19	35	$0.1183\angle -2.75^{\circ}$
DP31	35	DP1	35	$0.1183\angle -2.75^{\circ}$
DP18	35	DP1	35	$0.1183\angle -2.75^{\circ}$
DP19	35	DP19	35	$0.1183\angle -2.75^{\circ}$
DP19	35	DP1	35	$0.1183\angle -2.75^{\circ}$
DP1	35	DP1	35	$0.1183\angle -2.75^{\circ}$
DP9	35	DP18	35	$0.1183\angle -3.04^{\circ}$
DP9	35	DP31	35	$0.1183\angle -3.04^{\circ}$
DP9	35	DP19	35	$0.1183\angle -3.04^{\circ}$
DP9	35	DP1	35	$0.1183\angle -3.04^{\circ}$
DP9	35	DP9	35	$0.1183\angle -3.32^{\circ}$

It can be seen from **Table 1** that the main excitation bus at the 518 Hz resonant frequency point is DP31, HP20, DP19, HP1 and DP23. The bus DP31 is the inlet bus of the fracturing station, and the bus DP20, DP19 and DP1 are the inlet bus of the drilling rig. They are all connected to the platform DP23 through the transmission line, indicating that the resonant frequency point has an impact on the DP31 fracturing station and the DP20, DP19, DP1 and DP23 drilling stations.

It can be seen from **Table 1** that the main excitation bus at the 719 Hz resonant frequency point is DP31, DP18, DP19, DP1 and DP9, which indicates that the influence area of this resonant frequency point is involved in the DP31 fracturing station and the DP18, DP19, DP1 and DP9 drilling stations.

5. Conclusions

In this paper, the mathematical model of the internal components of the shale gas field distribution network considering the characteristics of the electric fracturing pump and the electric drill is established, and the main methods of harmonic resonance analysis are introduced. According to the different operating conditions of a shale gas field, the mode analysis method is used to analyze the problem, and the conclusions are as follows:

1) In the shale gas field, under the influence of the 5, 7, 13, 15 and 35, 37 harmonics in the frequency converter of the compressor platform, electric rig platform and electric fracturing pump platform, the resonant impedance value of the platform is large, which is easy to induce the harmonic resonant overvoltage of the power grid.

2) Due to the change of electrical circuit under different operating conditions, the resonant frequency points in the oilfield distribution network are mainly related to transmission line parameters, transformers and frequency converters. When the rectifier pulse number of frequency converters increases, the resonant frequency points increase significantly.

Conflicts of Interest

The authors declare no conflicts of interest regarding the publication of this paper.

References

[1] Nie, H.K., He, Z.L. and Liu, G.X. (2020) Status and Direction of Shale Gas Exploration and Development in China. *Journal of China University of Mining & Technology*, **49**, 13-35.

[2] Hu, S.J., Li, J.L. and Xu, H.H. (2008) Analysis of Converter Configuration for Direct-Drive Wind Power System with PMSG. *Electric Power Automation Equipment*, **28**, 77-81.

[3] Peng, J.W., Zhou, Q., Dai, Q.P., *et al.* (2016) Development Status and Analysis of Domestic Large-Scale Fracturing Equipment. *China Petroleum Machinery*, **44**, 82-86.

[4] Nie, R.G., Cai, M.J., Mao, L.J., *et al.* (2019) Effect of Fracturing Conditions on

the Stress Distribution of Shale Gas Well Casing. *China Petroleum Machinery*, **47**, 139-146.

[5] Zhao, X.P., Li, Z.B., Sun, F.D., *et al*. (2015) Research Status and Development Direction of Fracturing Truck. *Natural Gas and Oil*, **33**, 56-58.

[6] Ma, Z., Zhao, Z.G., Sun, Y.Y., *et al*. (2019) Key Technology and Development Prospect of New Generation Low Voltage DC Power Supply System. *Automation of Electric Power System*, **43**, 12-22.

[7] Liu, Y., Liu, C.H. and Fang, Q. (2019) Series-Connected Multilevel Voltage Disturbance Generator with Cascaded H-Bridge. *Power Electronics*, **53**, 114-117.

[8] Du, S.T. (2015) Key Technologies of Harmonic Suppression and Reactive Power Compensation. China University of Mining and Technology, Beijing.

[9] Liu, X.X. (2019) Research on Control Strategy of Grid-Connected Inverter Based on Improved Adaptive Delay Filtering. Harbin Institute of Technology, Harbin.

[10] Liu, X.Z. (2018) Harmonic Analysis and Treatment of Low Voltage Power Grid in Oilfield. *Electric World*, **59**, 33-35.

[11] Rahmani, S., Hamadi, A. and Al-Haddad, K. (2011) A Lyapunov-Function-Based Control for a Three-Phase Shunt Hybrid Active Filter. *IEEE Transactions on Industrial Electronics*, **59**, 1418-1429. https://doi.org/10.1109/TIE.2011.2163370

[12] Sasaki, H. and Machida, T. (1971) A New Method to Eliminate AC Harmonic Currents by Magnetic Flux Compensation-Considerations on Basic Design. *IEEE Transactions on Power Apparatus & Systems*, PAS-90, 2009-2019. https://doi.org/10.1109/TPAS.1971.292996

[13] Akagi, H., Kanazawa, Y. and Nabae, A. (2008) Instantaneous Reactive Power Compensators Comprising Switching Devices without Energy Storage Components. *IEEE Transactions on Industry Applications*, **IA-20**, 625-630. https://doi.org/10.1109/TIA.1984.4504460